Check for updates

Theobromine cocrystals with monohydroxybenzoic acids – synthesis, X-ray structural analysis, solubility and thermal properties†

Mateusz Gołdyn, [iD] * Daria Larowska, [iD]
Weronika Nowak and Elżbieta Bartoszak-Adamska [iD]

Theobromine, an organic compound from the purine alkaloid group, is much less soluble in polar solvents than its analogues, *i.e.* caffeine and theophylline, that is why it has been used as an active pharmaceutical ingredient (API) model in cocrystal preparation. A series of theobromine (**TBR**) cocrystallization processes from solutions with such coformers as 2-hydroxybenzoic acid (**2HBA**), 3-hydroxybenzoic acid (**3HBA**) and 4-hydroxybenzoic acid (**4HBA**) were carried out. In addition, neat grinding and liquid-assisted grinding were performed. The obtained cocrystals **TBR·2HBA** and **TBR·3HBA** as well as **TBR·2(4HBA)·H₂O** cocrystal monohydrate have been characterized by single crystal X-ray diffraction (SXRD), PXRD, UV-vis and STA (TGA/DSC) analyses. In all cases no proton transfer from the acid molecule to the imidazole nitrogen atom in theobromine was observed. TBR–acid heterosynthons are sustained by N···H–O interactions, where proton donors in **TBR·2HBA** and **TBR·3HBA** are carboxylic groups, and in **TBR·2(4HBA)·H₂O** the proton donor is the hydroxyl group of the acid molecule. In each cocrystal, TBR–TBR homosynthon $R_2^2(8)$ formation by N–H···O hydrogen bonds was observed. Acid–acid dimers are created only in the crystal lattice of **TBR·2(4HBA)·H₂O**. In the obtained cocrystals, similar supramolecular synthons were observed, such as in theophylline and caffeine cocrystals with the same coformers. C–H···O and π···π forces present in the described structures are responsible for 2D and 3D structure stabilization.

1. Introduction

The term "cocrystal" was used for the first time by Friedrich Wöhler in 1844 for quinhydrone, which consists of quinone and hydroquinone.[1] Cocrystals can be defined as homogeneous solids, composed of two or more substances (molecular and/or ionic) with a well-defined stoichiometric ratio, except simple salts and solvates. Their components have to be solids under ambient conditions.[2] In 2004, a subgroup of cocrystals was defined, where one of the components is an active pharmaceutical ingredient (API).[3] A new drug has to undergo a series of clinical trials, before it is placed on the market. Unfortunately, a lot of medicines (60–70%), which have good pharmacological properties, are characterized by poor aqueous solubility, which results in poor bioavailability.[4–6] In this case, improvement of the physicochemical properties such as solubility, stability, permeability or tabletability is crucial from the perspective of drug companies. The long times needed for introducing drugs on the market are usually connected with higher costs for pharmaceutical companies. A lot of methods like particle size reduction,[7] nanoparticle formation,[8] encapsulation[9] self-emulsifying drug delivery system (SEDDS),[10] salt formation,[11] complexation,[12] *etc.* can be used to improve the solubility of APIs in water. Moreover, cocrystallization of APIs with selected coformers is also used to improve the medicine's properties.[13] Cafcit (caffeine citrate),[14,15] Steglatro (ertugliflozin L-pyroglutamic acid)[16,17] and Lexapro (escitalopram oxalate)[18,19] are examples of medicine cocrystals. When it comes to the advantages of this method, APIs can exist in a stable crystalline form and their pharmacological activity is maintained while improving the physicochemical properties.

Theobromine is an organic compound, which belongs to the purine alkaloid group. It is present in cacao, yerba mate, kola nut, the guarana berry and the tea plant.[20] It is one of the metabolites formed in the human liver as a result of caffeine demethylation.[21] It affects the nervous system (cAMP

Faculty of Chemistry, Adam Mickiewicz University, Uniwersytetu Poznańskiego 8, 61-614 Poznań, Poland. E-mail: mateusz.goldyn@amu.edu.pl
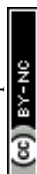
deactivation). It is a vasodilator and heart stimulant and it has diuretic properties.[22] For these reasons, it can be classified as an API but currently it is rarely used in the pharmaceutical industry. Although the theobromine molecule is structurally similar to paraxanthine, theophylline and caffeine, it is less soluble in water than them (0.33 g L^{-1} for theobromine, 1 g L^{-1} for paraxanthine, 7.4 g L^{-1} for theophylline, and 21.6 g L^{-1} for caffeine).[23] That is why theobromine was chosen as an API model for cocrystallization and as a result, its solubility in water can be improved. Monohydroxybenzoic acids were used as coformers, because they have proton-donor groups. Our choice is also related to an earlier use of these coformers for theophylline and caffeine cocrystallization (Fig. 1).[24,25]

In this paper, two cocrystals of theobromine (**TBR**) with 2-hydroxybenzoic acid (**2HBA**) and 3-hydroxybenzoic acid (**3HBA**), and a cocrystal hydrate with 4-hydroxybenzoic acid (**4HBA**) were reported.

All of these solids were obtained by slow evaporation from different solutions and they were analyzed by a single-crystal X-ray diffraction method. Steady-state UV-vis spectroscopy was used to determine the cocrystal solubility. Additionally, simultaneous thermal analysis (STA) measurement was carried out.

2. Experimental section

2.1. Materials

TBR (99%) was purchased from Swiss Herbal Institute. 2HBA (≥99%), 3HBA (99%) and 4HBA (≥99%) were obtained from Sigma-Aldrich. Hydroxybenzoic acids were used for cocrystallization without purification. Methanol was purchased from Chempur and ethanol from Stanlab. In all absorption experiments, Millipore distilled water (18 MΩ cm) was used.

2.2. Crystallographic database CSD search

To date, 31 different structures containing theobromine have been reported and they are available in the Cambridge Structural Database.[26] 10 of them contain carboxylic acid, such as 5-chlorosalicylic acid (CSATBR), oxalic acid (GORGUR), trifluoroacetic acid (HIJYAB), malonic acid (HIJYEF), gallic acid (MUPPET), acetic acid (NURYUV), salicylic acid (RUTHEV), anthranilic acid (ZIZRUX and ZIZRUX01), and 4-hydroxy-3-methoxybenzoic acid (ZOYBOG). Only five of them are composed of theobromine and a benzoic acid derivative: CSATBR, MUPPET, RUTHEV, ZIZRUX, and ZOYBOG. The ConQuest program was used for searching deposited structures containing theobromine.[26,27]
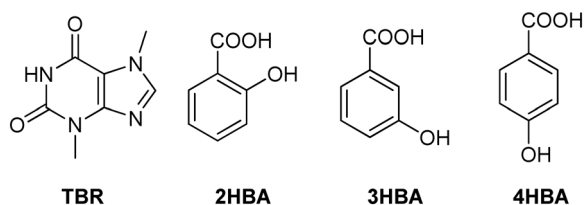

Fig. 1   Theobromine and monohydroxybenzoic acids.

2.3. Cocrystal preparation

2.3.1. Cocrystallization by slow evaporation from solution. Single crystals of **TBR·2HBA** and **TBR·3HBA** were obtained by slow evaporation from ethanol–water solution, and **TBR·2(4HBA)·H$_2$O** crystals from methanol–water solution. We used stoichiometric ratios of theobromine and the particular monohydroxybenzoic acid. TBR (16.1 mg, 0.09 mmol) with 2HBA (12.5 mg, 0.09 mmol), TBR (17.5 mg, 0.097 mmol) with 3HBA (13.4 mg, 0.097 mmol) and TBR (13.5 mg, 0.075 mmol) with 4HBA (20.7 mg, 0.15 mmol) were dissolved by heating and stirring, respectively. Monocrystals were obtained by slow evaporation of filtrates under ambient conditions within 3–5 days.

2.3.2. Cocrystallization by grinding. Substance cogrinding was carried out in stainless steel milling jars, where the stoichiometric amounts of theobromine with the given acid and two 6 mm stainless steel balls were placed inside. TBR (16.0 mg, 0.089 mmol) with 2HBA (12.5 mg, 0.091 mmol) and TBR (17.8 mg, 0.099 mmol) with 3HBA (13.7 mg, 0.099 mmol) were subjected to neat grinding, respectively. TBR (12.0 mg, 0.067 mmol) and 4HBA (18.5 mg, 0.134 mmol) were coground with the addition of 20 μl of water. Milling was performed using an oscillatory ball mill Retsch MM300 for 45 minutes at a frequency of 25 Hz.

2.4. Single-crystal X-ray diffraction (SXRD)

X-ray diffraction data were collected on an Oxford Diffraction SuperNova diffractometer equipped with a CuKα radiation source (λ = 1.54178 Å) and with a Cryojet cooling system. CrysAlisPro[28] and CrysAlisRed[29] were used for data collection and data reduction, respectively. Multi-scan absorption correction was applied to the diffraction data.[30] Olex2 software was used as an interface to facilitate the solution, refinement and structural analysis.[31] The structures were solved using intrinsic phasing with SHELXT-2015 and were refined with SHELXL-2015 software.[32] For non-hydrogen atoms, refinements were carried out with anisotropic atomic displacement parameters. All hydrogen atoms were derived from a difference Fourier map and they were refined isotropically. In **TBR·2(4HBA)·H$_2$O**, hydrogen atoms of two carboxyl groups are disordered over two positions and they were refined with restraints (occupancies 0.5 for H1C and H2C atoms, 0.25 for H1D and 0.75 for H2D atoms). The extinction coefficient was applied in the refinement of **TBR·2HBA** and **TBR·3HBA** structures. The crystallographic data and refinement details are presented in Tables 1 and 2.

2.5. Powder X-ray diffraction (PXRD)

Powder samples of components and cocrystals synthesized by grinding and by slow evaporation from solution were measured on an Oxford Diffraction Xcalibur diffractometer with a MoKα radiation source (λ = 0.71073 Å) at room temperature. The main goal of using the grinding method was to test this technique as an alternative way for this cocrystal synthesis. Experimental conditions: scanning intervals, 5–50° (2θ); step size, 0.01°; and time per step, 0.5 s. CrysAlisPro[28] was used for data collection. The experimental and calculated powder

Table 1 Cocrystal detection wavelengths

	Detection wavelength (λ_{det})
TBR·2HBA	320
TBR·3HBA	310
TBR·2(4HBA)·H$_2$O	300

patterns from the crystal structures were analyzed using Kdif software.[33]

2.6. Solubility studies of cocrystals by steady-state absorption spectroscopy

Steady-state UV-vis spectroscopy was used to determine the cocrystal solubility in distilled water. The powdered samples of cocrystals obtained by cocrystallization from solution were used for measurements. UV-vis absorption spectra were recorded using a two-beam spectrometer Cary 100 UV-vis scanning from 200 to 800 nm with 1 nm increments. Quartz cells with an optical length of 10 mm were used. Calibration curves of every cocrystal were prepared (Fig. S1†). Substance concentrations *versus* absorbance of the substance at detec-

tion wavelength (Table 1) were plotted. A linear relationship was obtained and the slope was calculated from the graph.

To determine the solubility of the cocrystals, saturated aqueous solutions of each were prepared. The absorbance at detection wavelength (λ_{det}) was measured and the concentration of the substance was calculated by applying the following relationship:

$$[\text{substance}] = \frac{\text{absorbance at detection wavelength}\,(\lambda_{det})}{\text{slope}} \quad (1)$$

2.7. Simultaneous thermal analysis (STA)

The thermal properties of the samples were characterized using a STA analyser (Perkin-Elmer STA6000). The sample measurements were carried out under a nitrogen atmosphere from room temperature to 400 °C at 10 °C min^{-1}.

3. Results and discussion

In this paper, three solids containing theobromine and monohydroxybenzoic acids are presented. This dimethyl-xanthine cocrystallizes with 2HBA and 3HBA (1:1) as co-

Table 2 Crystallographic data and experimental details for **1**, **2** and **3** cocrystals

	1	**2**	**3**
	TBR·2HBA	**TBR·3HBA**	**TBR·2(4HBA)·H$_2$O**
Deposition number	1934751	1934758	1934759
Molecular formula	C$_7$H$_8$N$_4$O$_2$·C$_7$H$_6$O$_3$	C$_7$H$_8$N$_4$O$_2$·C$_7$H$_6$O$_3$	C$_7$H$_8$N$_4$O$_2$·2(C$_7$H$_6$O$_3$)·H$_2$O
Formula weight, g mol^{-1}	318.29	318.29	474.43
Crystal system	Triclinic	Monoclinic	Triclinic
Space group	$P\bar{1}$	$P2_1/c$	$P\bar{1}$
a, Å	6.8096(2)	6.4812(2)	7.0166(2)
b, Å	7.9530(3)	23.7503(7)	12.4761(4)
c, Å	14.0826(4)	9.3288(3)	24.6450(8)
α, °	94.042(2)	90	99.639(3)
β, °	103.561(2)	101.841(3)	91.740(3)
γ, °	103.726(3)	90	99.464(3)
V, Å^3	713.78(4)	1405.44(8)	2094.29(12)
Z, Z'	2, 1	4, 1	4, 2
$F(000)$	332	664	992
D_x, g cm^{-1}	1.481	1.504	1.505
Radiation, Å	1.54184	1.54184	1.54184
μ, mm^{-1}	0.975	0.990	1.02
T, K	150.0(1)	150.0(1)	130.0(1)
Crystal size, mm^3	0.57 × 0.20 × 0.18	0.26 × 0.11 × 0.09	0.21 × 0.11 × 0.05
2θ range for data collection, °	6.514 to 152.442	7.444 to 152.012	7.290 to 153.214
Index ranges (h, k, l)	$-8 \leq h \leq 8$	$-6 \leq h \leq 8$	$-8 \leq h \leq 8$
	$-10 \leq k \leq 9$	$-29 \leq k \leq 29$	$-15 \leq k \leq 14$
	$-17 \leq l \leq 15$	$-11 \leq l \leq 10$	$-30 \leq l \leq 30$
Collected reflections	14 874	8760	16 429
Independent reflections	2986 (R_{int} = 0.0287, R_{sigma} = 0.0184)	2911 (R_{int} = 0.0216, R_{sigma} = 0.0214)	8559 (R_{int} = 0.0302, R_{sigma} = 0.0369)
Reflections with $I > 2\sigma(I)$	2795	2627	7299
Data/restraints/parameters	2986/0/265	2911/0/265	8559/0/797
Final R indices with $I > 2\sigma(I)$	R_1 = 0.0352	R_1 = 0.0384	R_1 = 0.0452
	wR_2 = 0.0982	wR_2 = 0.1052	wR_2 = 0.1325
Final R indices with all data	R_1 = 0.0372	R_1 = 0.0437	R_1 = 0.0525
	wR_2 = 0.1003	wR_2 = 0.1086	wR_2 = 0.1388
GOF	1.046	1.162	1.067
Extinction coefficient	0.0061(13)	0.0013(3)	None
$\Delta\rho_{min}$, $\Delta\rho_{max}$, e Å^{-3}	−0.19, 0.28	−0.20, 0.21	−0.33, 0.33

Table 3 Calculated ΔpK_a values

Acid	$pK_{a\,acid}$	$\Delta pK_a{}^a$
2HBA	3.01	−3.92
3HBA	4.08	−4.99
4HBA	4.57	−5.48

^{a} $pK_{a\,base}$ (theobromine) is equal to −0.91.

crystals. A hydrate was formed by combination of TBR and 4HBA (1 : 2). The bond lengths of C–O and C=O indicate the carboxylic group geometry. The difference Fourier map clearly shows the position of the acidic hydrogen atom near the oxygen atom of the carboxyl group in 2HBA and 3HBA. There is no proton transfer from hydroxyl groups of the 4HBA molecules to the imidazole nitrogen atom of TBR (Table 3).

The ΔpK_a parameter, described by the following equation:

$$\Delta pK_a = pK_a(\text{base}) - pK_a(\text{acid}) \qquad (2)$$

allows prediction of salt or cocrystal formation.[34] The determined values of ΔpK_a are less than zero. So, there is a high probability that the combination of theobromine with monohydroxybenzoic acids would result in cocrystals.

3.1. Crystal structure of the investigated cocrystals

3.1.1. TBR·2HBA cocrystal. For the first time, a theobromine (**TBR**) 2-hydroxybenzoic acid (**2HBA**) cocrystal was obtained by F. Fischer *et al.* in 2015 by cocrystallization from

solution and by neat grinding.[35] The structure was refined to an R value of 10.16%. In the above paper, there is no description of hydrogen bonds present in **TBR·2HBA**. Therefore, we decided to repeat the cocrystallization and X-ray analysis to obtain satisfactory refinement parameters.

TBR·2HBA crystallizes in the triclinic space group $P\bar{1}$ with one **TBR** and one **2HBA** molecule in the asymmetric unit (Fig. 2a). Typical C–O and C=O bond lengths of the carboxylic group were observed (1.310(1) Å for C7–O2 and 1.233(2) Å for C7=O1), which confirmed the crystallochemical nature of this cocrystal. Each **TBR** molecule is hydrogen bonded to **2HBA** *via* O2–H2⋯N4 interaction (synthon III, Fig. 3 and Table 4). The *ortho*-hydroxyl group in **2HBA** participates in intramolecular hydrogen bonding O3–H3⋯O1 and six-membered ring $S_1^1(6)$ is formed. In the crystal lattice, a finite centrosymmetric four-component system was identified (Fig. 2b). In this system two molecules of **TBR** interact *via* N1–H1⋯O4^{ii} hydrogen bonds (synthon II).

TBR·2HBA tetramers are connected by C–H⋯O forces creating a 2D layer parallel to the crystallographic plane (2$\bar{1}$0). The oxygen atom of the *endo*-carbonyl group of **TBR** participates in C6–H6⋯O5^i hydrogen bonding (Table 4), which together with the COOH⋯N$_{imidazole}$ heterosynthon forms the $R_4^4(22)$ motif. Carbon atom C14 of the methyl group at the imidazole ring acts as a donor in C14–H14C⋯O3^{iv} interaction, which takes part in cyclic array $R_6^6(22)$ formation (Fig. 2b). Two **TBR** molecules in neighboring sheets are connected through C14–H14B⋯O4^{iv} hydrogen bonding. Layers are arranged in an offset manner and form stacks (Fig. 2c), which are held together by π(**TBR**)⋯π(**2HBA**) forces (Fig. 2d and Table 5).
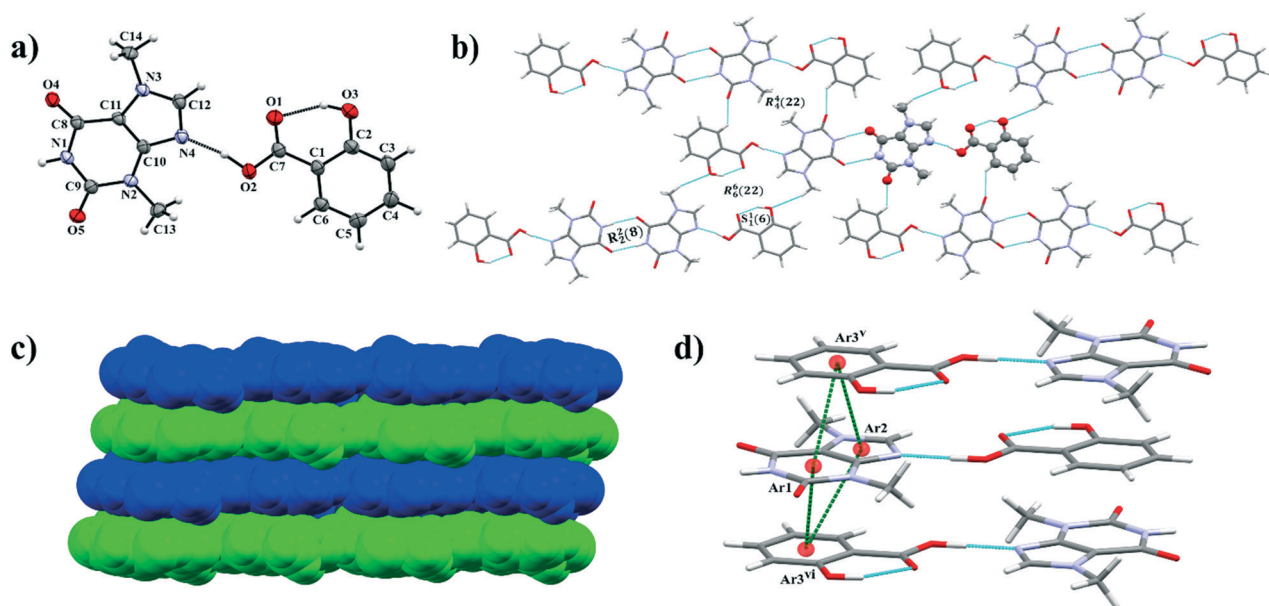
Fig. 2 a) ORTEP representation of the asymmetric unit of the **TBR·2HBA** cocrystal (thermal ellipsoids were drawn with the 50% probability level); b) molecular layer composed of four-component centrosymmetric systems of **TBR·2HBA** connected by C–H⋯O hydrogen bonds; structural motifs $S_1^1(6)$, $R_2^2(8)$, $R_4^4(22)$ and $R_6^6(22)$ are marked; c) neighboring **TBR·2HBA** sheets represented by green and blue colors interlinked *via* π⋯π interactions; d) representation of stacking interaction in the **TBR·2HBA** cocrystal (symmetry codes: (v) 1 − x, 1 − y, 1 − z, (vi) 2 − x, 1 − y, 1 − z).

3.1.2. TBR·3HBA cocrystal. The **TBR·3HBA** cocrystal, which crystallizes in the monoclinic space group $P2_1/c$, contains one **TBR** and one **3HBA** molecule in the asymmetric unit (Fig. 4a). The bond lengths of C–O (1.327(1) Å) and C=O (1.217(2) Å) confirmed that a cocrystal was obtained. In the crystal lattice, four-component centrosymmetric motif $R_4^4(26)$ composed of two **TBR** and two **3HBA** molecules is observed (Fig. 4b). This alkaloid is hydrogen bonded to two **3HBA** molecules by O2–H2···N4 (synthon III) and O3–H3···O5[iii] (synthon V) hydrogen bonds (Fig. 3 and Table 4). **TBR–TBR** dimers $R_2^2(8)$ are held by N1–H1···O4[ii] (synthon II) interaction, where the *exo*-carbonyl of **TBR** is involved in this formation.

The components of this cocrystal are arranged in ribbons parallel to the ($\bar{1}52$) and ($15\bar{2}$) crystallographic planes, which are inclined by γ = 100.6(1)° and form the "zigzag" sheet (Fig. 5a) by C5–H5···O3[i] interactions between **3HBA** molecules (Fig. 4c). The 1D ribbons form stacks, which are sustained by $\pi(\textbf{TBR})\cdots\pi(\textbf{TBR})$ and $\pi(\textbf{TBR})\cdots\pi(\textbf{3HBA})$ forces (Fig. 5b and Table 5). The average distance between neighboring layers is equal to 3.159(1) Å. The distance between

Fig. 3 Theobromine synthons observed in the described cocrystal structures.

Table 4 Hydrogen bond parameters for the described cocrystals

Cocrystal	D–H···A	D–H [Å]	H···A [Å]	D···A [Å]	D–H···A [°]
TBR·2HBA	C6–H6···O5[i]	0.99(2)	2.42(2)	3.146(2)	130(1)
	N1–H1···O4[ii]	0.87(2)	1.96(2)	2.835(1)	175(2)
	C14–H14B···O4[iii]	0.99(2)	2.55(2)	3.387(2)	142(2)
	C14–H14C···O3[iv]	0.99(2)	2.72(2)	3.646(2)	157(2)
	O3–H3···O1	0.92(2)	1.75(2)	2.587(1)	149(2)
	O2–H2···N4	1.05(2)	1.60(3)	2.635(1)	168(2)
Symmetry codes: (i) −x + 1, −y, −z + 1; (ii) −x + 1, −y, −z; (iii) −x + 1, −y + 1, −z; (iv) −x + 2, −y + 2, −z + 1					
TBR·3HBA	C5–H5···O3[i]	0.98(2)	2.85(2)	3.716(2)	148(2)
	N1–H1···O4[ii]	0.93(2)	1.84(2)	2.760(2)	173(2)
	O3–H3···O5[iii]	0.89(3)	1.93(3)	2.806(2)	169(3)
	O2–H2···N4	0.98(3)	1.75(3)	2.722(2)	177(3)
Symmetry codes: (i) x, −y + 1/2, z + 1/2; (ii) −x + 3, −y + 1, −z + 1; (iii) −x + 1, −y + 1, −z					
TBR·2(4HBA)·H2O	O1–H1E···O4A[i]	0.87(3)	1.93(3)	2.798(2)	173(3)
	O1–H1F···O5A[ii]	0.85(4)	2.13(4)	2.926(2)	156(4)
	O2A–H2A···O1B	0.89(4)	1.68(4)	2.564(2)	172(4)
	O3A–H3A···O1	0.87(3)	1.82(3)	2.683(2)	174(3)
	O2B–H2B···O1A	0.90(4)	1.78(4)	2.683(2)	176(4)
	O3B–H3B···N4A	0.93(3)	1.83(3)	2.742(2)	167(3)
	C5B–H5B···O2A[ii]	0.94(3)	2.43(3)	3.308(2)	155(2)
	C6B–H6B···O1B[ii]	0.94(3)	2.60(3)	3.395(2)	143(2)
	C5D–H5D···O2C[iv]	0.96(3)	2.40(3)	3.253(2)	147(2)
	C6D–H6D···O1D[iv]	0.98(2)	2.53(2)	3.344(2)	141(2)
	O2C–H2C···O1D	0.84(6)	1.74(6)	2.580(2)	177(4)
	O3C–H3C···O2	0.91(4)	1.73(4)	2.635(2)	173(3)
	O2D–H2D···O1C	0.72(5)	1.95(5)	2.660(2)	170(5)
	O3D–H3D···N4B	0.87(3)	1.95(3)	2.804(2)	169(3)
	N1B–H1B···O5B[iii]	0.89(3)	1.98(3)	2.864(2)	175(2)
	N1A–H1A···O5A[vi]	0.85(3)	2.01(3)	2.861(2)	178(2)
	O2–H2E···O5B[iv]	0.84(4)	2.08(4)	2.884(2)	163(3)
	O2–H2F···O4B[i]	0.85(3)	1.93(3)	2.781(2)	173(3)
	C13A–H13F···O3D[iv]	0.99(3)	2.76(3)	3.703(3)	158(2)
	C13B–H13B···O3B[iv]	0.96(2)	2.60(2)	3.535(2)	164(2)
	C14A–H14D···O4A[vii]	1.00(3)	2.56(2)	3.252(2)	127(2)
	C14B–H14A···O4B[v]	1.02(3)	2.63(3)	3.347(2)	128(2)

Symmetry codes: (i) x + 1, y, z + 1; (ii) −x + 2, −y + 1, −z + 2; (iii) −x − 1, −y + 1, −z; (iv) −x, −y + 1, −z + 1; (v) −x − 1, −y, −z; (vi) −x + 1, −y + 1, −z + 1; (vii) −x + 1, −y, −z + 1
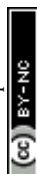
Table 5 Stacking interaction geometry in the described cocrystals

Cocrystal	ArM	ArN	ArM⋯ArN[a] [Å]	Dihedral angle[b] [°]	Interplanar distance[c] [Å]	Offset[d] [Å]
TBR·K2HB	Ar1	Ar3[v]	3.454(1)	2.35(1)	3.337(1)	0.89(1)
	Ar2	Ar3[v]	3.578(1)	1.96(1)	3.348(1)	1.26(1)
	Ar1	Ar3[vi]	3.633(1)	2.35(1)	3.332(1)	1.45(1)
	Ar2	Ar3[vi]	3.714(1)	1.96(1)	3.322(1)	1.66(1)
Symmetry codes: (v) $1 - x, 1 - y, 1 - z$, (vi) $2 - x, 1 - y, 1 - z$						
TBR·K3HB	Ar1	Ar1[iv]	3.318(1)	0	3.226(1)	0.78(1)
	Ar2	Ar1[iv]	3.664(1)	2.12(1)	3.198(1)	1.79(1)
	Ar2	Ar3[v]	3.756(1)	5.52(1)	3.224(1)	1.93(1)
Symmetry codes: (iv) $2 - x, 1 - y, 1 - z$, (v) $1 + x, y, z$						
TBR·2(K4HB)·H₂O	Ar2A	Ar3C	3.925(1)	10.35(1)	3.088(1)	2.42(1)
	Ar2B	Ar3A[viii]	3.708(1)	4.25(1)	3.353(1)	1.58(1)
Symmetry codes: (viii) $-2 + x, y, -1 + z$						

[a] The distance between the ring centroids. [b] The angle between aromatic ring planes. [c] The distance between the ArN plane to the ArM centroid. [d] The distance between ArM and ArN projected onto the ring plane M.

equivalent **TBR:3HBA** is equal to 11.875(1) Å, determined as a half (1/2 W) of the O1⋯O1$^{x,-1+y,z}$ distance (Fig. 5a).

3.1.3. TBR·2(4HBA)·H₂O cocrystal hydrate. Theobromine (**TBR**) and 4-hydroxybenzoic acid (**4HBA**) cocrystallize as a monohydrate in the triclinic space group $P\bar{1}$. The asymmetric unit contains two hydrate systems (**I** and **II**, Fig. 6a). Each of the hydrates forms a 1D ribbon with the same hydrogen

Fig. 4 a) ORTEP representation of the asymmetric unit of the **TBR·3HBA** cocrystal (thermal ellipsoids were plotted with the 50% probability level); b) molecular ribbon composed of structural units $R_4^4(26)$ connected by N–H⋯O hydrogen bonds, which in turn take part in $R_2^2(8)$ cyclic array formation; c) C–H⋯O interactions between acid molecules occurring on the sheet bend (Fig. 5a).
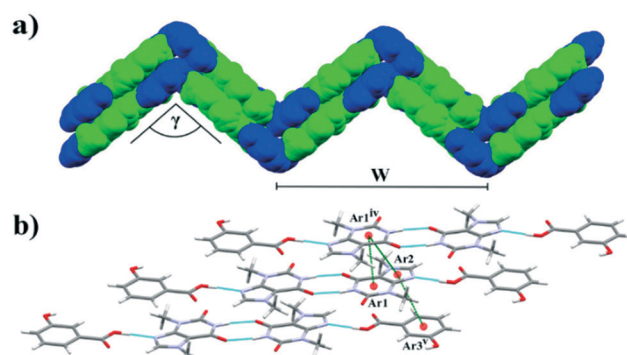
bond architecture (Fig. 6b). In this system, we can distinguish **TBR–TBR** and **4HBA–4HBA** dimers $R_2^2(8)$ held by N–H⋯O (synthon I, Fig. 3) and O–H⋯O hydrogen bonds, respectively (Table 4). The hydroxyl group of one **4HBA** molecule is connected with the imidazole nitrogen atom of **TBR** through O–H⋯N interaction (synthon IV), and the hydroxyl group of the second **4HBA** molecule is a proton donor for the oxygen atom from the water molecule (O–H⋯O interaction). Hydrogen atoms of the solvent are hydrogen bonded to the oxygen atom from the *exo*-carbonyl group of one **TBR** molecule (synthon VIII) and from the *endo*-carbonyl group of the second **TBR** molecule (synthon VII) *via* O–H⋯O hydrogen bonds, respectively. In this way, together with N–H⋯O forces, motifs $R_3^2(8)$ are formed. In the 1D ribbon, C–H⋯O interactions are present, where aromatic carbon atoms of **4HBA** molecules are proton donors for two oxygen atoms of the neighboring acid–acid dimer.

By means of C–H⋯O hydrogen bonds, neighboring 1D polymers in **TBR·2(4HBA)·H₂O** are arranged in layers (Fig. 6b). The methyl groups at the imidazole ring are proton donors for oxygen atoms of the *exo*-carbonyl groups in **TBR**. In the second interaction, the imidazole carbon atom is a

Fig. 5 a) The "zigzag" sheet of **TBR·3HBA** formed by C–H⋯O interactions between ribbons, which are stacked by π⋯π interactions, b) representation of stacking interaction in **TBR·3HBA** (green and blue colors represent **TBR** and **3HBA** molecules, respectively).
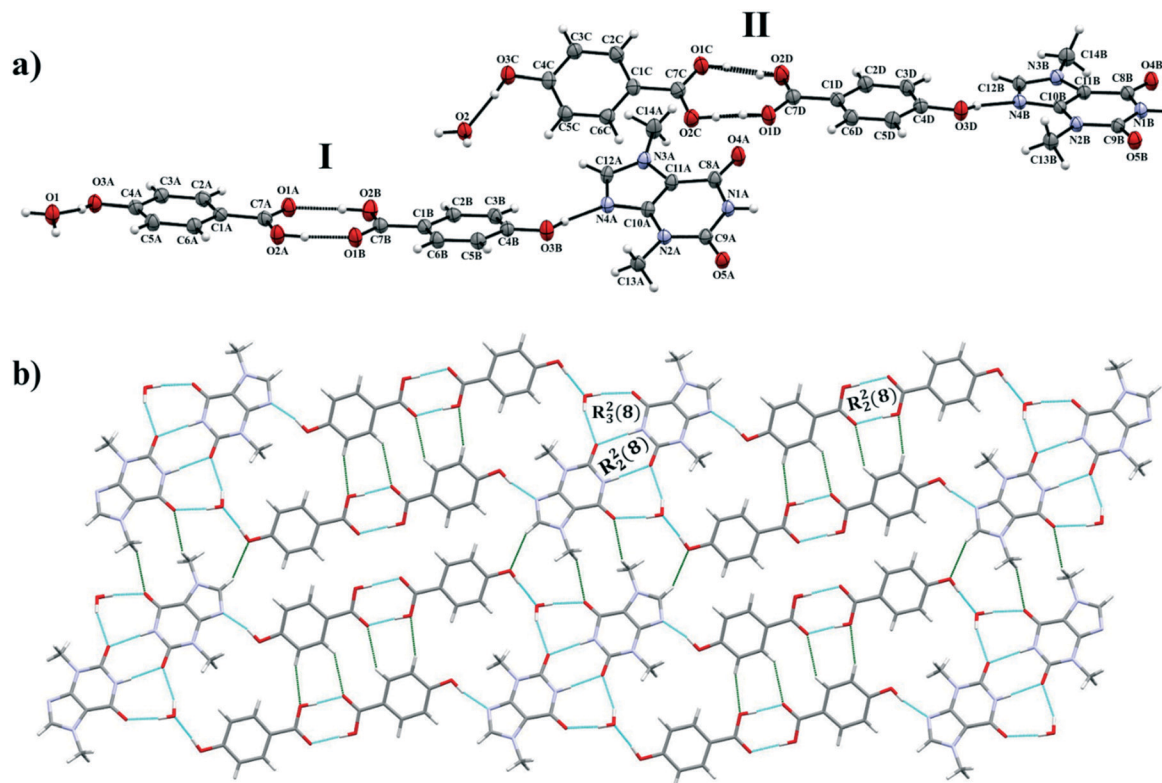
Fig. 6 a) ORTEP representation of the **TBR·2(K4HB)·H₂O** asymmetric unit, which is composed of two hydrate systems (**I** and **II**; thermal ellipsoids were drawn with the 50% probability level); b) molecular layer of hydrate **I** formed by C–H⋯O interactions (green color) between ribbons; in ribbons C–H⋯O hydrogen bonds were identified between aromatic carbon atoms, which are proton donors for oxygen atoms participating in acid–acid dimer formation.

proton donor for the **4HBA** hydroxyl group connected to the water molecule. π(**TBR**)⋯π(**K4HB**) interactions (Fig. 7b and Table 5) are responsible for creating stacks (Fig. 7a).

3.2. Comparison of supramolecular synthons found in theobromine, caffeine and theophylline cocrystals with monohydroxybenzoic acids

Molecules of theobromine (3,7-dimethylxanthine), theophylline (1,3-dimethylxanthine) and caffeine (1,3,7-trimethyl-

Fig. 7 a) Molecular layers of **TBR·2(4HBA)·H₂O**, which are held by π⋯π interactions (blue and green colors indicate the layers composed of **I** and **II** hydrate systems, respectively); b) representation of π(**TBR**)⋯π(**K4HB**) interactions in the **TBR·2(4HBA)·H₂O** cocrystal hydrate.

xanthine) differ by the number and the position of the methyl group(s).

Three nitrogen atoms of the caffeine molecule are substituted by methyl groups, therefore this purine molecule cannot form any CAF–CAF homodimer by strong classical hydrogen bonds. In turn, in theophylline one kind of TPH–TPH homodimer $R_2^2(10)$ with the participation of C=O(endo-carbonyl) and N–H(imidazole) groups can be observed (Fig. 8E). However, in the theobromine molecule, there are two possibilities of TBR–TBR homosynthon $R_2^2(8)$ amide–amide formation via C=O(exo-carbonyl) or C=O(endo-carbonyl) together with the N–H(pyrimidine) group, respectively (Fig. 8B). The carboxylic acid–carboxylic acid homosynthon is popular[37] (Fig. 8A), but in the presence of the alkaline imidazole nitrogen atom this hydrogen-bonded moiety is uncommon.[38] Below, the supramolecular synthons in theobromine cocrystals with monohydroxybenzoic acids are discussed and compared with theophylline and caffeine cocrystals with the same coformers (Table 6).

3.2.1. Purine alkaloid cocrystals with 2-hydroxybenzoic acid as a coformer. In the above alkaloid cocrystals with 2-hydroxybenzoic acid, according to Etter's rules,[39] first an intramolecular O–H⋯O hydrogen bond with an $S_1^1(6)$ motif is expected, which mainly stabilizes the carboxylic acid molecule (Fig. 8C). Consequently, cocrystal formation is only possible by intermolecular COOH⋯N_imidazole interactions
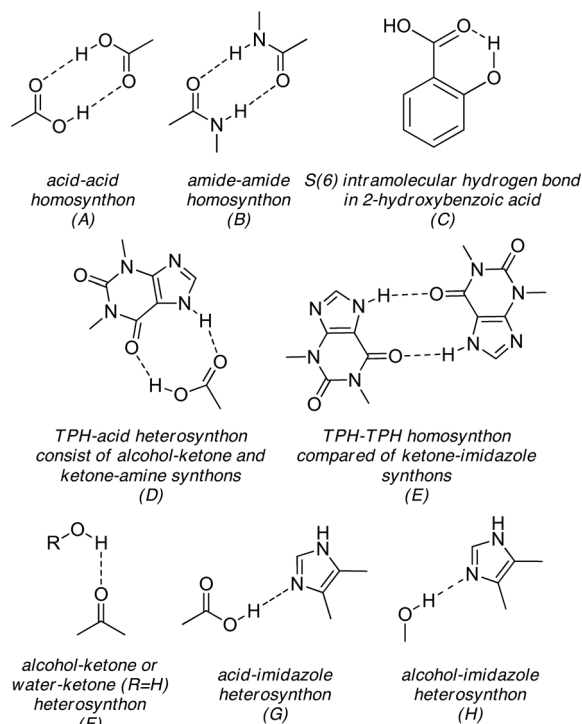
Fig. 8 (A–H) Supramolecular synthons present in the described theobromine, theophylline and caffeine cocrystals with monohydroxybenzoic acids as coformers. A, B, F and G motifs are some of the commonly studied and used synthons in crystal design.[37]

(Fig. 8G). In TBR·2HBA and TPH·2HBA cocrystals, one can also expect TBR–TBR and TPH–TPH homosynthons, respectively (Fig. 8B and E).

In the CAF·2HBA cocrystal, the alkaloid and acid molecule form a two-molecular complex by a COOH···N hydrogen bond (Fig. 8G). The remaining interactions are weak stacking interactions (1D and 2D structures) and C–H···O hydrogen bonds (3D structure).[25] In the case of the TPH·2HBA cocrystal, the COOH···N$_{imidazole}$ heterosynthon, the TPH–TPH homosynthon R$_2^2$(10) (Fig. 8E) and the acid–acid heterosynthon held through O–H(o-hydroxyl)···O=C(carboxyl) hydrogen bonds (Fig. 8F) are responsible for the 1D molecular ribbon formation. In turn, 2D and 3D architectures of TPH·2HBA are stabilized by C–H···O and π-stacking interactions, respectively.[24] In both structures, the intramolecular O–H···O interaction in salicylic acid was observed. (Fig. 8C).

In the TBR·2HBA crystal lattice, TBR–TBR R$_2^2$(8) dimers hydrogen bonded via N–H(pyrimidine)···O=C(exo-carbonyl) interactions (Fig. 8B), TBR–2HBA dimers sustained by

COOH···N$_{imidazole}$ hydrogen bonds (Fig. 8G) and the S$_1^1$(6) cyclic array in the 2HBA acid (Fig. 8C) are in line with expectations. These synthons are some of the most common hydrogen-bonded motifs present in organic cocrystals.[37]

3.2.2. Purine alkaloid cocrystals with 3-hydroxybenzoic acid as a coformer. The hydroxyl group in the 3-hydroxybenzoic acid is in the meta-position, so it cannot take part in intramolecular hydrogen bond formation. This group can probably be a proton acceptor from the endo- or exo-carbonyl oxygen atoms in alkaloid molecules. In CAF·3HBA[25] and TPH·3HBA[24] cocrystals, the hydroxyl groups in acid molecules are proton donors for the endo-carbonyl groups in caffeine and theophylline molecules, respectively (Fig. 8F). The COOH···N$_{imidazole}$ heterosynthon (Fig. 8G) is present in both complexes. In the TPH·3HBA cocrystal, theophylline molecules form TPH–TPH homodimers by C=O(exo-carbonyl)···H–N(imidazole) hydrogen bonds (Fig. 8E).

The structural motifs in TBR·3HBA are similar to those aforementioned in CAF and TPH analogues. The theobromine molecules form homosynthons held by N–H(pyrimidine)···O=C(exo-carbonyl) hydrogen bonds (Fig. 8B), TBR–3HBA systems are held by COOH···N$_{imidazole}$ interactions (Fig. 8G) and the meta-hydroxyl group in the acid is a proton donor for the oxygen atom in the endo-carbonyl group of this xanthine molecule (Fig. 8F). So, based on the caffeine and theophylline complexes with 3-hydroxybenzoic acid, it was possible to predict which synthons would be responsible for the crystal lattice arrangement in the theobromine cocrystal with the investigated coformer. The 2D and 3D networks of these cocrystals are sustained by C–H···O and stacking interactions.

3.2.3. Purine alkaloid cocrystals with 4-hydroxybenzoic acid as a coformer. In the case of the 4-hydroxybenzoic acid, there are 3 combinations of this coformer with caffeine.[24,25,36] In each of these combinations, the N$_{imidazole}$···HOOC heterosynthon can be observed (Fig. 8G). In CAF·2(4HBA), oxygen atoms in the para-hydroxyl group of the acid molecules are proton donors for the endo- and exo-carbonyl oxygen atoms in caffeine, however in 2(CAF)·4HBA this group is a proton donor only for the endo-carbonyl oxygen atom (Fig. 8F). In the CAF·4HBA·H$_2$O complex, the water molecule is a proton acceptor from the para-hydroxyl group in 4HBA and it is also a proton donor for the endo- and exo-carbonyl groups in the alkaloid molecule (Fig. 8F for the water molecule). What is more, in the CAF·2(4HBA) cocrystal, acid molecule pairs are connected via O–H(carboxyl)···O=C(carboxyl) hydrogen bonds. In

Table 6 Purine alkaloid cocrystals with 2-hydroxy-, 3-hydroxy- and 4-hydroxybenzoic acids as coformers

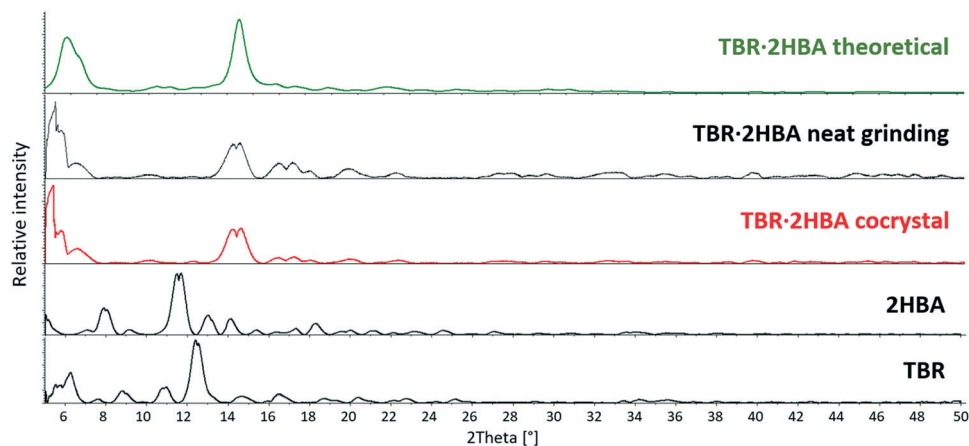|	2HBA	3HBA	4HBA
Theobromine (TBR)	TBR·2HBA (RUTHEV,[35] this work)	TBR·3HBA (this work)	TBR·2(4HBA)·H$_2$O (this work)
Theophylline (TPH)	TPH·2HBA (KIGLES01)[24]	TPH·3HBA (DOPMUS)[24]	TPH·4HBA (DOPNAZ)[24]
Caffeine (CAF)	CAF·2HBA (XOBCAT01)[25]	CAF·3HBA (MOZCOU)[25]	2(CAF)·4HBA (MOZCUA)[25]
			CAF·2(4HBA) (MOZDAH)[25]
			CAF·4HBA·H$_2$O (LATBIT)[36]

Fig. 9 Comparison of powder X-ray diffraction patterns for theobromine, 2-hydroxybenzoic acid and the TBR·2HBA cocrystal.

TPH·4HBA, theophylline molecules are connected with one acid molecule by $N_{imidazole}\cdots HO$ interaction (Fig. 8H) and with the second one by O–H(carboxyl)$\cdots$O=C(*exo*-carbonyl) and C=O(carboxyl)$\cdots$H–N(imidazole) hydrogen bonds ($R_2^2(9)$ motif, Fig. 8D). Homosynthons are not observed in these cocrystals. Thus, it was difficult to predict whether the combination of theobromine and 4-hydroxybenzoic acid would result in a cocrystal or cocrystal hydrate, and what stoichiometry of substrates and which synthons would be responsible for the arrangement of these components in complex.

Theobromine and 4-hydroxybenzoic acid cocrystallize in a 1:2:1 stoichiometric ratio together with a water molecule and form a cocrystal hydrate. In this structure, we recognized two types of homosynthons, *i.e.* the TBR–TBR homodimer, which are held by C=O(*endo*-carbonyl)$\cdots$H–N(pyrimidine) hydrogen bonding (Fig. 8B) and the acid–acid homosynthon between two carboxylic groups (Fig. 8A). The imidazole nitrogen atom accepts a proton from the hydroxyl group of one acid molecule (Fig. 8H). In purine cocrystals with 2HBA and 3HBA, this synthon is not observed. The hydroxyl group of the second acid molecule is a proton donor to water molecule, which is in turn the donor of two protons to *endo*- and

exo-carbonyl oxygen atoms of two different theobromine molecules (Fig. 8F). The last motif was observed in CAF ·4HBA·H$_2$O.[36]

3.3. Powder X-ray diffraction

The powder diffractograms of theobromine (API), coformers (2-, 3- and 4-hydroxybenzoic acid) and the studied cocrystals were obtained (Fig. 9–11). The differences between the diffractograms of the substrates and the cocrystals are clearly visible. What is more, the similarity of the powder patterns for the cocrystal samples obtained by crystallization from the solution and the milling samples indicates that grinding is an alternative method for the preparation of the studied theobromine derivatives.

3.4. Steady-state UV-vis spectroscopy

3.4.1. UV-vis measurements. TBR is slightly soluble in water (0.33 g L^{-1}).[23] To improve its aqueous solubility, cocrystallization with highly soluble acids was performed. The solubility of the obtained cocrystals was determined and compared with the solubility of pure **TBR** (Table 7). The 3–6
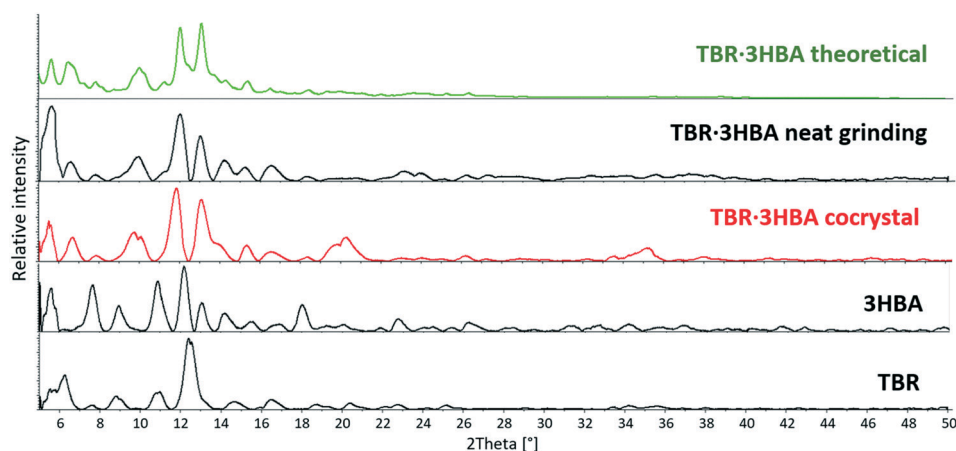

Fig. 10 Comparison of powder X-ray diffraction patterns for theobromine, 3-hydroxybenzoic acid and the TBR·3HBA cocrystal.
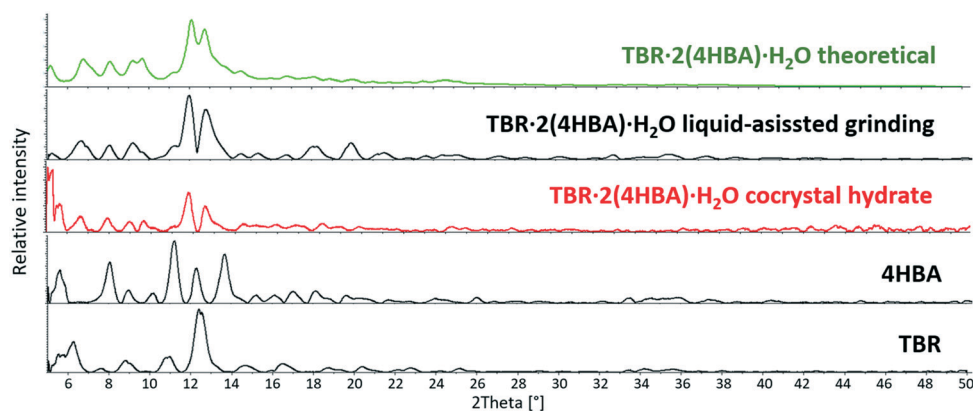
Fig. 11 Comparison of powder X-ray diffraction patterns for theobromine, 4-hydroxybenzoic acid and the TBR·2(4HBA)·H$_2$O cocrystal hydrate.

times enhancement of the theobromine solubility in relation to pure alkaloid was observed. Surprisingly, there is no relationship between the aqueous solubility of coformers and the enhancement of coformers.[40]

3.4.2. Solubility enhancement of theobromine in cocrystals and their crystal structure. The better solubility of the theobromine cocrystal with the *ortho*-hydroxybenzoic acid in comparison to that with the *meta* isomer can be explained by intermolecular interactions. Although both compounds crystallize in different space groups ($P\bar{1}$ and $P2_1/c$), their architecture is comparable. In TBR·2HBA and TBR·3HBA cocrystals, an identical $R_2^2(8)$ synthon is observed. Additionally, similar structural motifs $R_4^4(22)$ and $R_6^6(22)$ in TBR·2HBA and $R_4^4(26)$ in TBR·3HBA are recognized. The main difference between the crystal structures of these cocrystals is the strength of intermolecular interactions. In the first, more soluble cocrystal, the presented motifs are formed by O–H⋯N and weak C–H⋯O forces, whereas $R_4^4(26)$ systems in TBR·3HBA are stabilized by strong classical O–H⋯O/N hydrogen bonds. The theobromine solubility in the TBR·2(4HBA)·H$_2$O cocrystal hydrate is lower than that in TBR·2HBA and greater than that in TBR·3HBA. This may be due to the presence of a water molecule in the crystal lattice and more impact of strong hydrogen bonds on the molecular arrangement compared to TBR·2HBA.

3.5. Simultaneous thermal analysis (STA)

Fig. 12 shows the TGA and DSC curves of TBR·2HBA, TBR·3HBA and TBR·2(4HBA)·H$_2$O.

The presence of water in the TBR·2(4HBA)·H$_2$O crystal structure is evident from the DSC measurements. The first signal of the cocrystal appears at a temperature of about 113 °C. It can be assumed that the water molecules from the crystal structure are released. The second signal, at 215 °C, refers to the complete decomposition of the 4HBA molecules, and is in agreement with the melting point of pure 4HBA.[42] The signal at 315 °C is attributed to the decomposition of the TBR molecules. Because of the low mass content of water in the crystal structure, the weight loss in the TGA curve at about 113 °C is nearly unnoticeable. In the 104–250 °C temperature range, the loss of material reaches 32%. The second mass loss takes place in the temperature range of 250–325 °C.
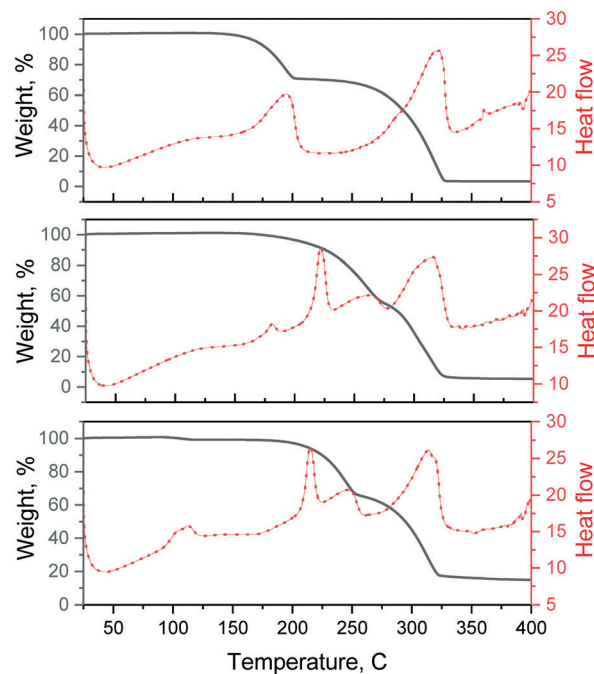

Fig. 12 The simultaneous thermal analysis (STA) curves of TBR·2HBA (top), TBR·3HBA (center) and TBR·2(4HBA)·H$_2$O (bottom). TG and DSC curves are represented by black and red colors, respectively.

Table 7 Solubility of theobromine cocrystals in water. The relative increase to TBR is shown in parenthesis

	Absorption solubility (g L^{-1})	Aqueous solubility of coformers (g L^{-1})
TBR·2HBA	2.07 (×6.3)	2.24 (ref. 41)
TBR·3HBA	1.06 (×3.2)	7.25 (ref. 42)
TBR·2(4HBA)·H$_2$O	1.56 (×4.7)	5 (ref. 43)

In the TBR·2HBA cocrystal, the first signal is observed at around 194 °C and in the TBR·3HBA cocrystal, it is at 223 °C. At these temperatures, the appropriate monohydroxybenzoic acids decompose. Since their decomposition temperature is higher than that of the pure acids (melting temperature of pure 2HBA – 158 °C and pure 3HBA – 202 °C).[42] It can be concluded that the 2HBA and 3HBA molecules are stabilized in the cocrystals. At these temperatures, a TBR·2HBA mass loss of approximately 30% can be observed in the TGA curve and the TBR·3HBA mass loss is higher and reaches about 45%, respectively. The second DSC signal is related to the theobromine decomposition.

4. Conclusions

Three solids consisting of theobromine and mono-hydroxybenzoic acids (*ortho*, *meta* and *para*) were synthesized. Good quality single crystals of TBR·2HBA, TBR·3HBA and TBR·2(4HBA)·H$_2$O were obtained by slow evaporation from solution and were characterized by the single-crystal X-ray diffraction method. It allowed us to prove the crystallochemical nature of the new cocrystals and redetermine the TBR·2HBA crystal structure.[35] Powder X-ray diffraction studies confirmed the successful green chemistry synthesis by grinding in a ball mill. Cocrystallization of theo-bromine improves its solubility in water approximately 6 times for the TBR·2HBA cocrystal, 5 times for the TBR·2(4HBA)·H$_2$O cocrystal hydrate and 3 times for the TBR·3HBA cocrystal. Additionally thermal analysis confirms the presence of water molecules in the crystal lattice of TBR·2(4HBA)·H$_2$O. In all of the compounds, the acids decompose first, followed by theobromine.

Structural analysis showed that strong hydrogen bonds play a key role in the molecular arrangement in the crystal lattice of the described theobromine derivatives. In this work, the supramolecular synthons observed in the theobromine cocrystals with monohydroxybenzoic acids were discussed and they were also compared to the structural motifs in the-ophylline and caffeine cocrystals with the same coformers. Generally, supramolecular heterosynthons are more preferred than homosynthons.[34] Our studies showed that in all of the investigated theobromine cocrystals with mono-hydroxybenzoic acids, the amide–amide homosynthon is present. Additionally, in the TBR·4HBA·H$_2$O cocrystal hydrate, the acid–acid homosynthon is formed. In comparison to the theophylline cocrystals with 2HBA and 3HBA as coformers, the alkaloid–alkaloid homosynthon (TPH–TPH) is observed. Caffeine molecules do not form homosynthons and only heterosynthons are present in their cocrystals with mono-hydroxybenzoic acids.

The oxygen atoms of the *exo*- and *endo*-carbonyl groups are good proton acceptors. In all of the described alkaloid complexes with monohydroxybenzoic acids, at least one of these groups is a proton acceptor from the hydroxyl group or water molecule in the case of the cocrystal hydrate. The imid-azole nitrogen atom accepts a proton from the carboxyl group

and only in two cases (TPH·4HBA and TBR·4HBA·H$_2$O) from the hydroxyl group. In all of the investigated structures, weak C–H···O hydrogen bonds and π-stacking interactions stabilize the 2D and 3D networks. The knowledge (based on the CSD data) about theophylline and caffeine cocrystals with mono-hydroxybenzoic acids allowed us to predict partially which su-pramolecular synthons would be responsible for the arrangement of theobromine and these acid molecules, when they form cocrystals.

Conflicts of interest

There are no conflicts to declare.

Acknowledgements

References

1 F. Wöhler, *Justus Liebigs Ann. Chem.*, 1844, **51**, 145–163.

2 S. Aitipamula, R. Banerjee, A. K. Bansal, K. Biradha, M. L. Cheney, A. R. Choudhury, G. R. Desiraju, A. G. Dikundwar, R. Dubey, N. Duggirala, P. P. Ghogale, S. Ghosh, P. K. Goswami, N. R. Goud, R. R. K. R. Jetti, P. Karpinski, P. Kaushik, D. Kumar, V. Kumar, B. Moulton, A. Mukherjee, G. Mukherjee, A. S. Myerson, V. Puri, A. Ramanan, T. Rajamannar, C. M. Reddy, N. Rodriguez-Hornedo, R. D. Rogers, T. N. G. Row, P. Sanphui, N. Shan, G. Shete, A. Singh, C. C. Sun, J. A. Swift, R. Thaimattam, T. S. Thakur, R. Kumar Thaper, S. P. Thomas, S. Tothadi, V. R. Vangala, N. Variankaval, P. Vishweshwar, D. R. Weyna and M. J. Zaworotko, *Cryst. Growth Des.*, 2012, **12**, 2147–2152.

3 N. K. Duggirala, M. L. Perry, Ö. Almarsson and M. J. Zaworotko, *Chem. Commun.*, 2016, **52**, 640–655.

4 N. J. Babu and A. Nangia, *Cryst. Growth Des.*, 2011, **11**, 2662–2679.

5 S. Y. K. Fong, A. Ibisogly and A. Bauer-Brandl, *Int. J. Pharm.*, 2015, **496**, 382–391.

6 F. Kesisoglou, S. Panmai and Y. Wu, *Adv. Drug Delivery Rev.*, 2007, **59**, 631–644.

7 J. C. Chaumeil, *Methods Find. Exp. Clin. Pharmacol.*, 1998, **20**(3), 211–215.

8 P. Sheth, H. Sandhu, D. Singhal, W. Malick, N. Shah and M. Serpil Kislalioglu, *Curr. Drug Delivery*, 2012, **9**, 269–284.

9 H. Griesser, A. Schwenger and C. Richert, *ChemMedChem*, 2017, **12**, 1759–1767.

10 C. Stillhart and M. Kuentz, *J. Pharm. Biomed. Anal.*, 2012, **59**, 29–37.

11 D. Gupta, D. Bhatia, V. Dave, V. Sutariya and S. Varghese Gupta, *Molecules*, 2018, **23**, 1719.

12 A. Ascenso, R. Guedes, R. Bernardino, H. Diogo, F. A. Carvalho, N. C. Santos, A. M. Silva and H. C. Marques, *AAPS PharmSciTech*, 2011, **12**, 553–563.

13 O. N. Kavanagh, D. M. Croker, G. M. Walker and M. J. Zaworotko, *Drug Discovery Today*, 2019, **24**, 796–804.

14 Pharmaceutical Society of Great Britain, *The British Pharmaceutical Codex*, Pharmaceutical Society of Great Britain, 1907.

15 S. Karki, T. Friščić, W. Jones and W. D. S. Motherwell, *Mol. Pharmaceutics*, 2007, **4**, 347–354.

16 P. Bowles, S. J. Brenek, S. Caron, N. M. Do, M. T. Drexler, S. Duan, P. Dubé, E. C. Hansen, B. P. Jones, K. N. Jones, T. A. Ljubicic, T. W. Makowski, J. Mustakis, J. D. Nelson, M. Olivier, Z. Peng, H. H. Perfect, D. W. Place, J. A. Ragan, J. J. Salisbury, C. L. Stanchina, B. C. Vanderplas, M. E. Webster and R. M. Weekly, *Org. Process Res. Dev.*, 2014, **18**, 66–81.

17 R. Santra, B. K. R. Bhogala, C. H. Khanduri and Sun Pharmaceutical Industries Limited, *US Pat.* App. 15/576452, 2018.

18 L. Peikova, M. Manova, S. Georgieva and G. Petrova, *Biotechnol. Biotechnol. Equip.*, 2013, **27**, 4044–4047.

19 W. T. A. Harrison, H. S. Yathirajan, S. Bindya, H. G. Anilkumar and Missing Devaraju, *Acta Crystallogr., Sect. C: Cryst. Struct. Commun.*, 2007, **63**(2), o129–o131.

20 *Science*, http://xocoatl.org/science.htm (accessed on 17 June, 2019).

21 H. R. Ha, F. Follath, J. Chen and S. Krähenbühl, *Eur. J. Clin. Pharmacol.*, 1996, **49**, 309–315.

22 K. Izawa, Y. Amino, M. Kohmura, Y. Ueda and M. Kuroda, In *Comprehensive Natural Products II*, Elsevier, 2010, pp. 631–671.

23 J. K. Guillory, *J. Med. Chem.*, 2003, **46**, 4213–4213.

24 D.-K. Bučar, R. F. Henry, G. G. Z. Zhang and L. R. MacGillivray, *Cryst. Growth Des.*, 2014, **14**, 5318–5328.

25 D.-K. Bučar, R. F. Henry, X. Lou, R. W. Duerst, L. R. MacGillivray and G. G. Z. Zhang, *Cryst. Growth Des.*, 2009, **9**, 1932–1943.

26 C. R. Groom, I. J. Bruno, M. P. Lightfoot and S. C. Ward, *Acta Crystallogr., Sect. B: Struct. Sci., Cryst. Eng. Mater.*, 2016, **72**, 171–179.

27 I. J. Bruno, J. C. Cole, P. R. Edgington, M. Kessler, C. F. Macrae, P. McCabe, J. Pearson and R. Taylor, *Acta Crystallogr., Sect. B: Struct. Sci.*, 2002, **58**, 389–397.

28 Agilent (2014). *CrysAlis PRO. Agilent Technologies Ltd*, Yarnton, Oxfordshire, England.

29 Oxford Diffraction (2006). *CrysAlis RED. Oxford Diffraction Ltd*, Abingdon, Oxfordshire, England.

30 G. M. Sheldrick, (1996). *SADABS. Program for Empirical Absorption Correction*, University of Gottingen, Germany.

31 O. V. Dolomanov, L. J. Bourhis, R. J. Gildea, J. A. K. Howard and H. Puschmann, *J. Appl. Crystallogr.*, 2009, **42**, 339–341.

32 G. M. Sheldrick, *Acta Crystallogr., Sect. A: Found. Adv.*, 2015, **71**, 3–8.

33 https://www.fzu.cz/~knizek/kalvados/ (accessed on 21 June, 2019).

34 S. Kumar and A. Nanda, *Indian J. Pharm. Sci.*, 2017, **79**(6), 858–871.

35 F. Fischer, M. Joester, K. Rademann and F. Emmerling, *Chem. – Eur. J.*, 2015, **21**, 14969–14974.

36 S. Aitipamula, P. S. Chow and R. B. H. Tan, *CrystEngComm*, 2012, **14**, 2381.

37 M. K. Corpinot and D.-K. Bučar, *Cryst. Growth Des.*, 2018, **19**, 1426–1453.

38 D.-K. Bučar, R. F. Henry, X. Lou, R. W. Duerst, T. B. Borchardt, L. R. MacGillivray and G. G. Z. Zhang, *Mol. Pharmaceutics*, 2007, **4**, 339–346.

39 M. C. Etter, *Acc. Chem. Res.*, 1990, **23**, 120–126.

40 P. Sanphui and A. Nangia, *J. Chem. Sci.*, 2014, **126**(5), 1249–1264.

41 R. M. Dannenfelser and S. H. Yalkowsky, *Sci. Total Environ.*, 1991, **109–110**(C), 625–628.

42 *The Human Metabolome Database (HMDB)* (accessed on 23 June, 2019).

43 S. H. Yalkowsky and Y. He, *Handbook of Aqueous Solubility Data*, CRC Press, Boca Raton, 2003, p. 377.